Article:
Nourafkan, E, Asachi, M, Hu, Z et al. (2018) Synthesis of stable nanoparticles at harsh environment using the synergistic effect of surfactants blend. Journal of Industrial and Engineering Chemistry, 64. pp. 390-401. ISSN: 1226-086X

https://doi.org/10.1016/j.jiec.2018.04.002

Formation of Stable Nanoparticle Dispersions in High Temperature High Salinity Conditions by using the Synergistic Effect of Surfactants Blend

Ehsan Nourafkan[†], Maryam Asachi[†], Zhongliang Hu, Hui Gao[†], Dongsheng Wen[*,†,‡]

[†]Institute of Particle Science and Engineering, School of Chemical and Process Engineering, University of Leeds, Leeds, LS2 9JT, United Kingdom

[‡]School of Aeronautic Science and Engineering, Beihang University, Beijing, P.R.China

ABSTRACT

Producing stable nanoparticle dispersions that can withstand high temperature and high salinity (HTHS) is still presenting as a big challenge in the research community. A novel strategy to synthesize stable nanoparticles under harsh conditions is proposed in this work by using the synergistic effect of a surfactant mixture. Long-term stable iron oxide nanoparticles (IONPs) under HTHS conditions were produced and stabilized by two different surfactant classes, i.e. sulfonate surfactant for high temperature resistance and ethoxylated alcohol surfactant for high salinity resistance. Blend of commercial surfactants of internal olefin sulfonate (IOS) and alcohol alkoxy sulfate (AAS) with ethoxylated alcohol (EA) were evaluated for their ability to improve the stability of IONPs in API brine plus 2 wt% of $MgCl_2$ for the first time. The results prove the feasibility of the new strategy. A critical length was determined for hydrocarbon tail of IOS, where NPs become destabilized beyond the critical value. A mechanism for formation of NPs in the presence of mixed micelles of anionic IOS/nonionic EA surfactants with different EO chain lengths was proposed. Such a strategy could be used for large-scale production of stable NPs under HTHS conditions that suitable for many applications including enhanced oil recovery.

KEYWORDS: *Iron oxide nanoparticles, high temperature, high salinity, enhanced oil recovery, phase behavior, Synergistic effect.*

1. INTRODUCTION

With the growth in energy demand and the decline of oil production from conventional methods, new techniques such as nanotechnology have attracted intensive attention to enhance oil recovery (EOR). Several studies have revealed the promising properties of nanoparticles (NPs) for EOR application[1-4], and other subsurface applications including map well connectivity, reservoir imaging and characterization[5-7]. Small size and long-term stability of NPs in hard conditions of a reservoir are highly beneficial for these applications, which is still a high challenging problem. Some of the outstanding works about the synthesis of NPs under high temperature-high salinity are briefly reviewed here.

Lim et al.[8] synthesized super paramagnetic NPs with iron oxide cores and contiguous gold shells under 150 mM ionic strengths of NaCl with different coating materials of pluronic, poly ethylene glycol, dextran and phosphate buffered saline (BSA). They reported that the best steric stabilization was obtained for BSA and Pluronic components. Bagaria et al.[9,10] functionalized iron oxide NPs by a series of sulfonated components and block copolymers under API brine conditions at 90 °C. The results showed that iron oxide NPs coated with poly (2-methyl-2-acrylamido propane sulfonate-co-acrylic acid) were stable in API brine at both room temperature and 90 °C for up to one month. Ranka et al.[11] proposed using polyampholytes, instead of polyelectrolytes for functionalizing of NP. They stated polyelectrolyte shrank, while a polyampholyte swelled under high ionic media and high temperature. Despite of these efforts, there is still a big gap in producing stable NP dispersions under high salinity and high temperature conditions, and the selection of suitable surfactants is a major hurdle.

The two surfactant families that widely used for surfactant flooding are sulfates and sulfonates. The sulfonate surfactants are more stable than sulfates at higher temperature. The internal olefin sulfonate (IOS) has some advantage properties (e.g. twin-tailed, high solubilization activity, high temperature resistance and low cost) which make them as potential candidates for surfactant flooding. Screening of commercial IOS and alcohol alkoxy sulfate (AAS) surfactant for EOR application at high salinity and high temperature has been experimentally investigated by Barnes et al.[12], Wu et al.[13], Jang et al.[14], and Puerto et al.[15]. Barnes et al.[16] evaluated the results IOS with different carbon numbers using improved phase behavior experimental methods and showed that IOS family of surfactants had good chemical

stability at higher temperatures (up to 150°C) and high solubilization of oil at their optimal salinities. However high critical micelle concentration (CMC) and limited salinity tolerance are the main drawbacks of anionic surfactant, which make them inappropriate for applying at high concentrations of divalent ions[17].

Nonionic ethoxylated surfactants are generally soluble in water, having low CMC and good stability in high salinity conditions[18] while they are not effective for high temperature condition[19]. Surfactants that have an ethoxylated group have tendency to pick up water molecules and hydrate, which could improve the solubility of this class of surfactants. While at higher temperature the ability of holding water molecules is declined due to the motion of the ethoxylated chain, resulting in the dehydration of surfactant[20]. On the other side anionic surfactant (especially with sulfonate hydrophilic group) has a good solubility in water and mostly stable in a high temperature conditions[21].

Previous researches have demonstrated the positive effect of addition of ethoxylated group (EO) to improve the salt tolerance of surfactant[21-23]. Puerto et al.[21] tested optimal salinity of both ethoxylated and propoxylated surfactants with various EO chain lengths at high temperature and high salinity by observing the phase behavior. They concluded ethoxylated surfactants exhibited optimal salinities with octane up to 21% NaCl at 120°C. Bansal and Shah[23,24] also showed that the salt concentration limit of every surfactant formulation was enhanced with the addition of ethoxylated surfactant. They observed that the thickness of ionic media around mixed micelles is decreased by increasing ethoxylated surfactant molecules. A synergistic effect of different mixed surfactant systems for EOR applications is subsequently proposed[25,26].

In this work, we propose a novel strategy to synthesize stable NPs at harsh conditions by using the synergistic effect of surfactants. As an example study, iron nanoparticles (IO NPs) are produced and stabilized by a surfactant mixture, including anionic IOS to address the high temperature tolerance, and nonionic EA surfactant to provide resistance to high salinity at API brine level. The effect of hydrocarbon tail length of IOS and ethoxylated group (EO) length on both mixed micelles characterization and IO NP functionalization are investigated to optimize the stabilization effect. Careful characterization of formed NPs is conducted including morphology, stability and interfacial properties. The results prove the feasibility of the new

strategy, which can be used for large-scale production of stable NPs under high salinity and high temperature conditions that suitable for many applications including EOR.

2. EXPERIMENTAL PROCEDURE

2.1. MATERIALS AND CHARACTERIZATION

Ethoxylated alcohol of Neodol 91-8 (C9-11/8 EO), Neodol 25-12 (C12-15/12 EO), IOS with nominal ranges of O332 (C15-18), O342 (C19-23), O242 (C20-24), O352 (C24-28) and AAS (J071, C12-13/7 EO) were provided by Shell Company. Ethoxylated alcohol N23-7 (C12-13/7 EO) was purchased from Mistral chemical Company (UK). Analytical grade materials including calcium chloride, magnesium chloride, sodium chloride, sodium hydroxide, ferric chloride ($FeCl_3$), ferrous chloride ($FeCl_2$) were purchased from Sigma-Aldrich. Mineral oil (Keratech 24 MLP, viscosity on file is 24 mPa.s at 40 °C) was purchased from Kerax Ltd (UK).

Phase Behavior of Surfactant Solution and IO NPs dispersion. One ml of solution containing surfactant blend or functionalized IO NPs in brine containing 8 wt.% NaCl, 2 wt.% $CaCl_2$ and 2 wt.% $MgCl_2$ which is called API brine, was put in a long glass pipette (3 mm internal diameter). One ml of n-Octane as oil phase was added to the glass pipette, then was sealed and finally was put in an oven at 70 °C for 3 weeks.

Stability of IO NPs dispersion. The stability of IO NPs over flocculation and sedimentation was characterized by recording the transmission of near-infrared light during the centrifugation of NPs by a dispersion analyzer centrifuge (LUMiSizer, Lum GmbH, Berlin, Germany). The solution (0.5 ml) was filled in a polycarbonate capillary cell and centrifuged for about 10 min at 2600 rpm (light factor 1, 25 ºC, 870 nm NIR LED), which is equivalent to one week in real conditions. The correlation between real time and centrifuge time is presented in “Calculation of the total measurement time for LUMiSizer 6110” part of the supplementary document.

Viscosity and Interfacial Tension (IFT). Goniometer (CAM 2008, KSV instruments Ltd. Finland) was used for IFT measurement for surfactant solution or NPs dispersion with mineral oil at 22 °C by an axisymmetric drop shape analysis (pendant drop method). Before each measurement the device was calibrated and the accuracy was checked by the IFT measurement

of pure water in air (~72 mNm^{-1}). The IFT values were obtained using the Young-Laplace equation. Viscosity was measured using a Physica Anton Paar rheometer, model MCR 301 (Cone plate CP75-1) at a shear range 10-1000 s^{-1} at 22 °C.

Zeta Potential and Hydrodynamic Size. Zeta potential and Hydrodynamic size of IO NPs or mixed micelles were measured with Malvern Zetasizer ZS instrument at 22 °C. Zeta potential was determined by the Smoluchowski model.

TEM and SEM-EDX. The morphology and size distribution of IO NP was analyzed by Transmission electron microscope (FEI Tecnai TF20 TEM). Elemental mapping of functionalized IO NPs were analyzed using a scanning electron microscope (FEI Quanta 650 FEG), which was equipped with X-Max energy dispersive X-ray detector (Oxford Instruments). The total time of 4 hour was considered for production of EDX map data with one minutes duration time per each frame.

Sulfur analyses: The sulfur element in functionalized IO NP was measured by combustion method by using Flash 2000 thermo Scientific.

2.2.SYNTHESIS OF IRON OXIDE NANOPARTICLES

Generally in ASP/SP flooding, the surfactant concentration usually is in the range of 0.2-3.0 wt. % range. In this study 0.001 g/ml was selected as the surfactant concentration in API brine in all experiments, which is higher than the CMC value of alcohol ethoxylated and IOS.

The initial IO NPs synthesis was performed using just IOS with different hydrocarbon tail length. After that the blend of sulfonate surfactant and ethoxylated alcohol with equal mass ratio was used. The synthesis of IO NPs was performed based on Massart co-precipitation method according to the following reaction[27].

$$FeCl_2 + 2\,FeCl_3 + 8NaOH \rightarrow Fe_3O_4 + 8NaCl + 4H_2O \quad (1)$$

Concentration of reactants for the synthesis of 500 ppm IO NP was estimated by stoichiometry. The concentration of ferrous chloride was chosen as 1.5 times of the stoichiometry value of ferric chloride. 2 ml Sodium hydroxide in brine (8 wt. % NaCl) with stoichiometry ratio was added drop wise to the surfactant solution as the precursor during a period of 10 minutes. The temperature of reaction was kept constant at 80 ºC using a hot water

bath. The mixture was stirred over 4 hours to reach the equilibrium at this temperature. Ultimately the NPs dispersion was put inside an oven at constant temperature of 70 ºC for one month without any mixing.

3. RESULT AND DISCUSSION

3.1.STABILITY ANALYSIS

First stage of screening surfactants was performed by observing the sedimentation behavior of NPs by naked eyes. It revealed that by increasing the tail length of sulphonate surfactant more than C20, the stability of IO NP was decreased (Figure S1). This may be attributed to the self-coiling or attractive tail-tail interaction of long alkyl tails of IOS, which takes place for hydrocarbon tail length longer than C20[28,29]. Therefore the O332, O342 were selected after the initial screening stage for further NPs synthesis. Moreover some trials of IO NP synthesis were performed using AAS (J071), which was suggested by the manufacture for high salinity condition applications[30]. The stability analysis of NPs containing blend of sulfonate surfactant (O332, O342, J071) and EA (N23-7, N91-8, N25-12) is shown in Figure 1.

a)

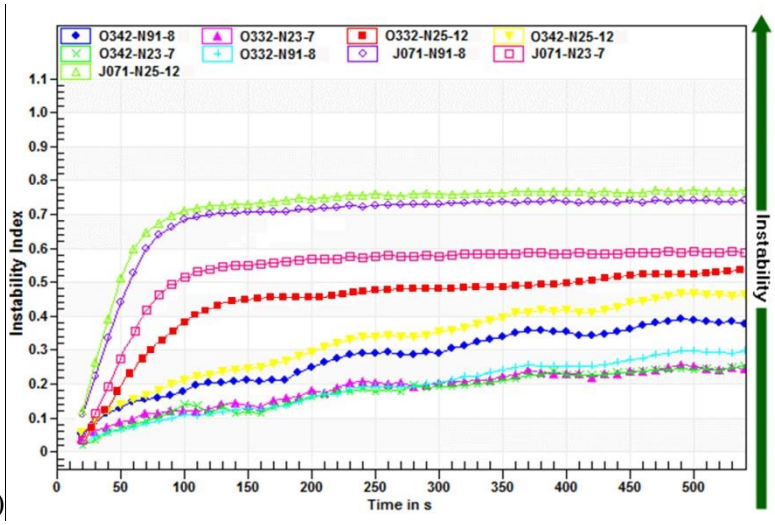

Figure 1. Trend of centrifuge dispersion analyzer for IO NP de-stability in API brine containing surfactants blend.

Figure 1 shows that IO NPs synthesized by IOS-N23-7 blend have the highest stability while IOS-N9-8 has second level of stability, which will be discussed in depth in “section 3-5”. The samples test tubes at the end of centrifuge operation and patterns of light transmission through them as a function of time is illustrated in Figure 2, which show that IOS-N23-7 ethoxylated

alcohol increase slower than other samples under the influence of the centrifugal force. Moreover NIR pattern shows higher agglomeration or flocculation of NPs for surfactant blend containing J071[31]. Figure S2 shows five stable IO NPs dispersions after 30 days immobility at 70 ºC which implies the excellent long-term stability of IO NPs.

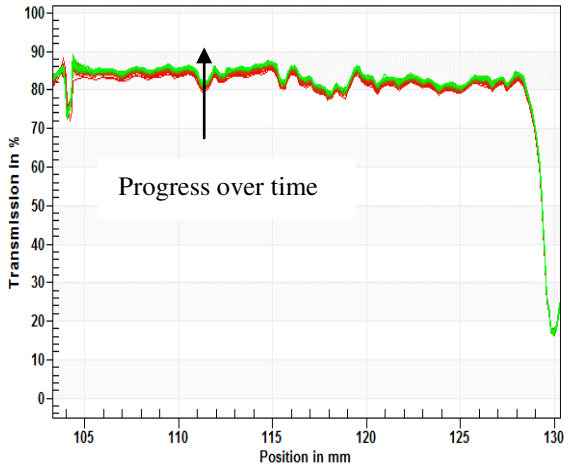

(a)

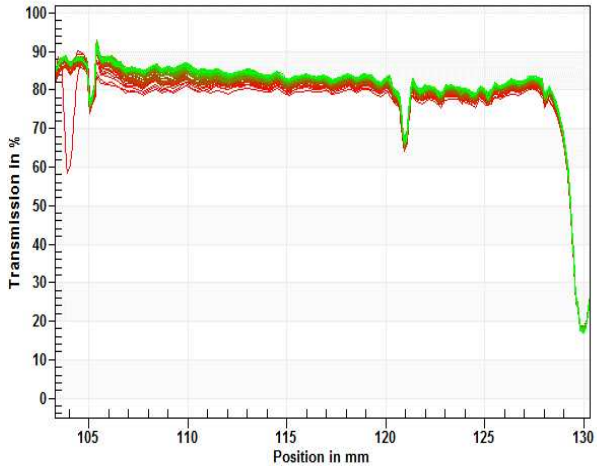

(b)

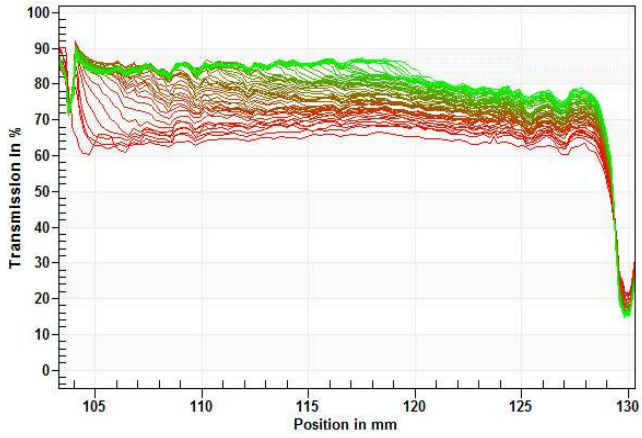

(c)

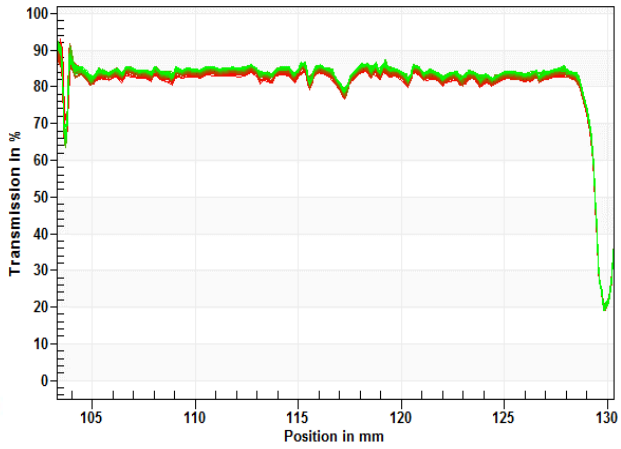

(d)

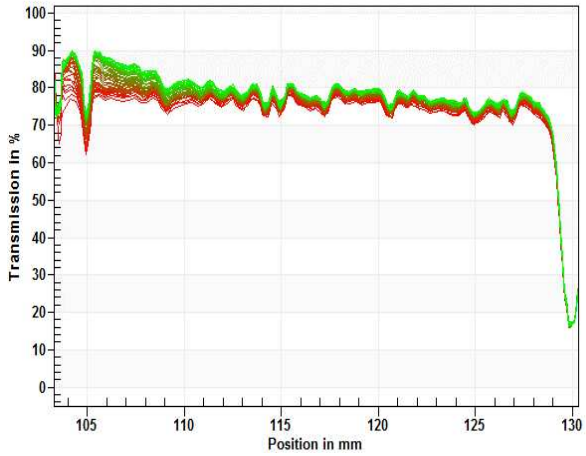
Transmission in %
Position in mm

(e)

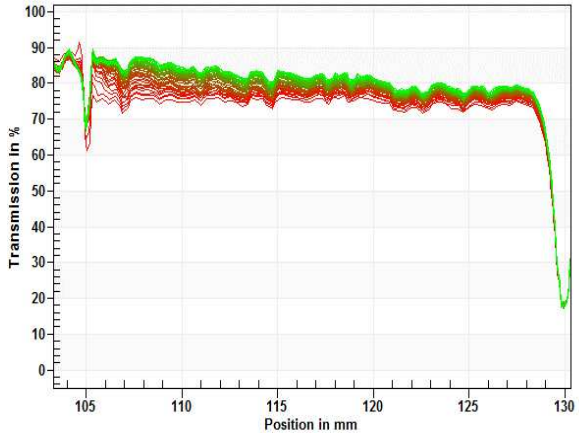
Transmission in %
Position in mm

(f)

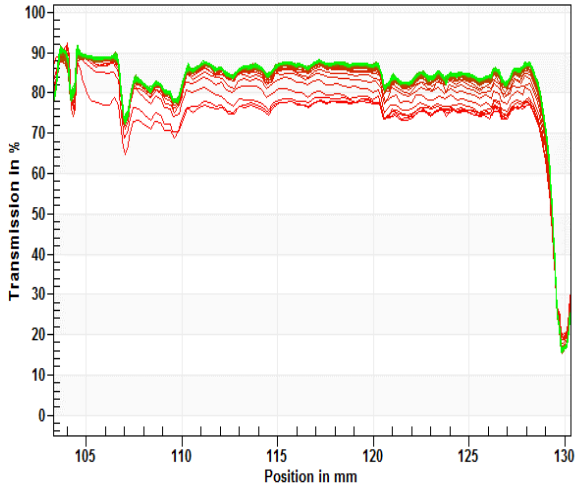
Transmission in %
Position in mm

(g)

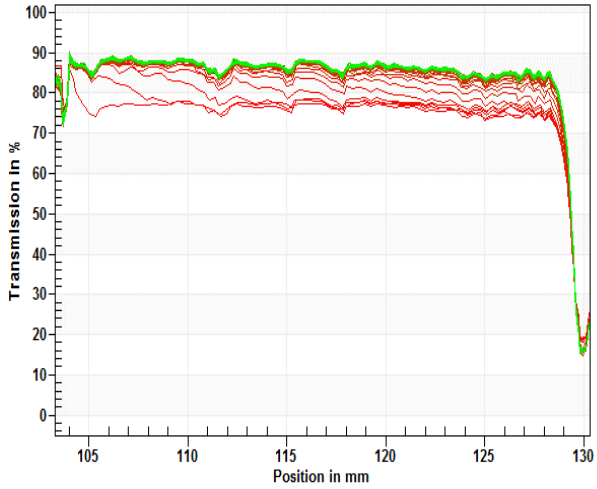
Transmission in %
Position in mm

(h)

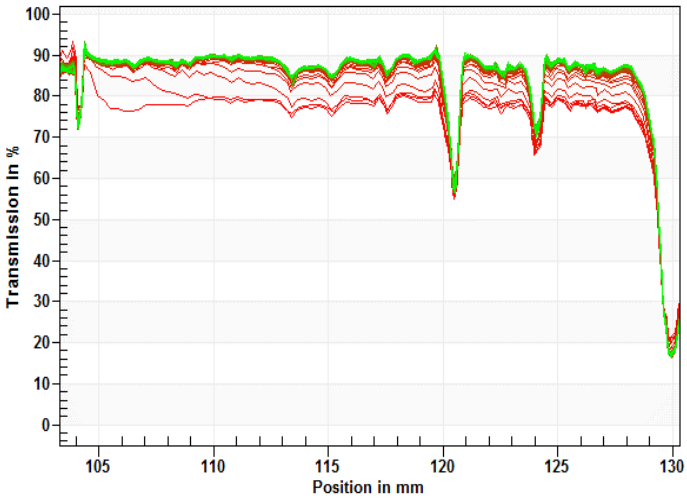
Transmission in %
Position in mm

(i)

(j) 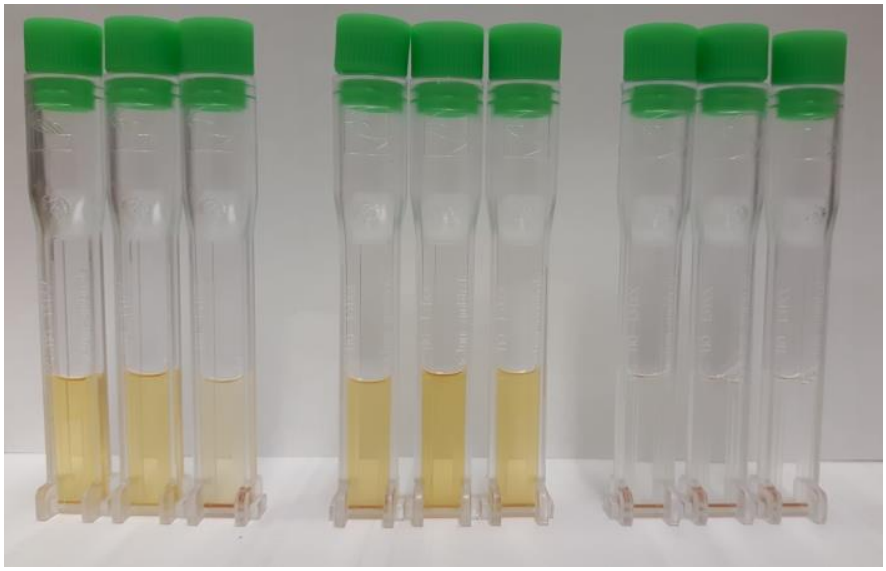

Figure 2. Patterns of light transmission through the test tube for (a) O332-N23-7, (b) O332-N91-8, (c) O332-N25-12, (d) O342-N23-7, (e)O342-N91-8, (f) O342-N25-12, (g)J071-N23-7, (h) J071-N91-8, (i) J071-N25-12 and (j) samples test tubes at the end of centrifuge operation.

3.2.EFFECT OF SALINITY ON MIXED MICELLES

The properties of mixed micelles of ethoxylated surfactant and sulfonate surfactant are much different from those of individual one, which affect the formation and stabilization of IO NPs. The surface charge density of a micelle is controlled by the mole fraction of the ionic surfactant in the mixed micelles. Ethylene oxide chains have effect on surface charge density, mobility and size of mixed micelles by sterically separating and screening ionic head of anionic surfactant[32]. In addition the shape, size and fractional charge of the mixed micelle greatly depend on the type and distribution of counterions inside the fluid. It has been suggested by Aswal and Goyal[33] that the size of cationic micelles increased in the presence of KBr salt in an aqueous solution by small-angle neutron scattering (SANS). Dynamic light scattering instrument as well-known powerful tool for surfactant size characterization was used for the measurement of hydrodynamic size of micelles at different salinities[34-36]. Table 1 represents hydrodynamic size of micelles in pure water and API brine.

Table 1. Hydrodynamic size of surfactant Micelles.

Surfactant micelle	O332	O342	N23-7	N91-8	N25-12	O332-N23-7	O332-N91-8	O332-N25-12	O342-N23-7	O342-N91-8	O342-N25-12
De-ionized water (nm)	3.91	5.6	8.64	5.31	7.87	3.12	2.75	2.92	3.93	2.96	3.37
API brine (nm)	125.6	128.4	9.01	7.95	8.69	34.22	15.49	11.25	24.10	14.47	10.09

According to Table 1, the size of micelles for pure IOS is increased dramatically in API brine; however for ethoxylated alcohol the difference in size is not major. This observation is attributed to the increase of the aggregation number of IOS's micelles. In fact counterions in API brine decrease the effective polar sulfonate head area of IOS in micelles, which lead to the rise of aggregation number. On the other hand there is not any intensive effect of counterions on EO group, which justifies the constant micelles size of EA surfactant in API brine.

For mixed micelles of IOS-EA in pure water, the size of O342-N25-12 is smaller than O342-N23-7 despite of longer EO chain (12 versus 7 in N23-7). Previous studies showed that hydrophobic core diameter decreased with increasing EO chain length[32,37]. The steric repulsion between the EO head groups led to an increase of hydrocarbon chain disorder and coiling. The increase of micelle size arising from longer EO chain layer thickness would be compensated by decreasing of hydrophobic core and consequently a reduction of the overall micelle size.

Another subtle but important point which outlined in the Table 1 is the relatively higher aggregation number and consequently larger hydrodynamic size of IOS-N23-7 blend comparing to IOS-N25-12 at API brine. Figure 3 showed a proposed schematic of IOS's mixed micelle in pure water and API brine. According to Figure 3a and b the thicker EO layer of N25-12 decreases the density of counterions around mixed micelles compared to N23-7. Therefore the charge neutralization in IOS-N23-7 blend is increased due to the counterion condensation at the surface of the micelles. Ultimately head group of IOS surfactant monomers occupy less space and hence the aggregation number is increased.

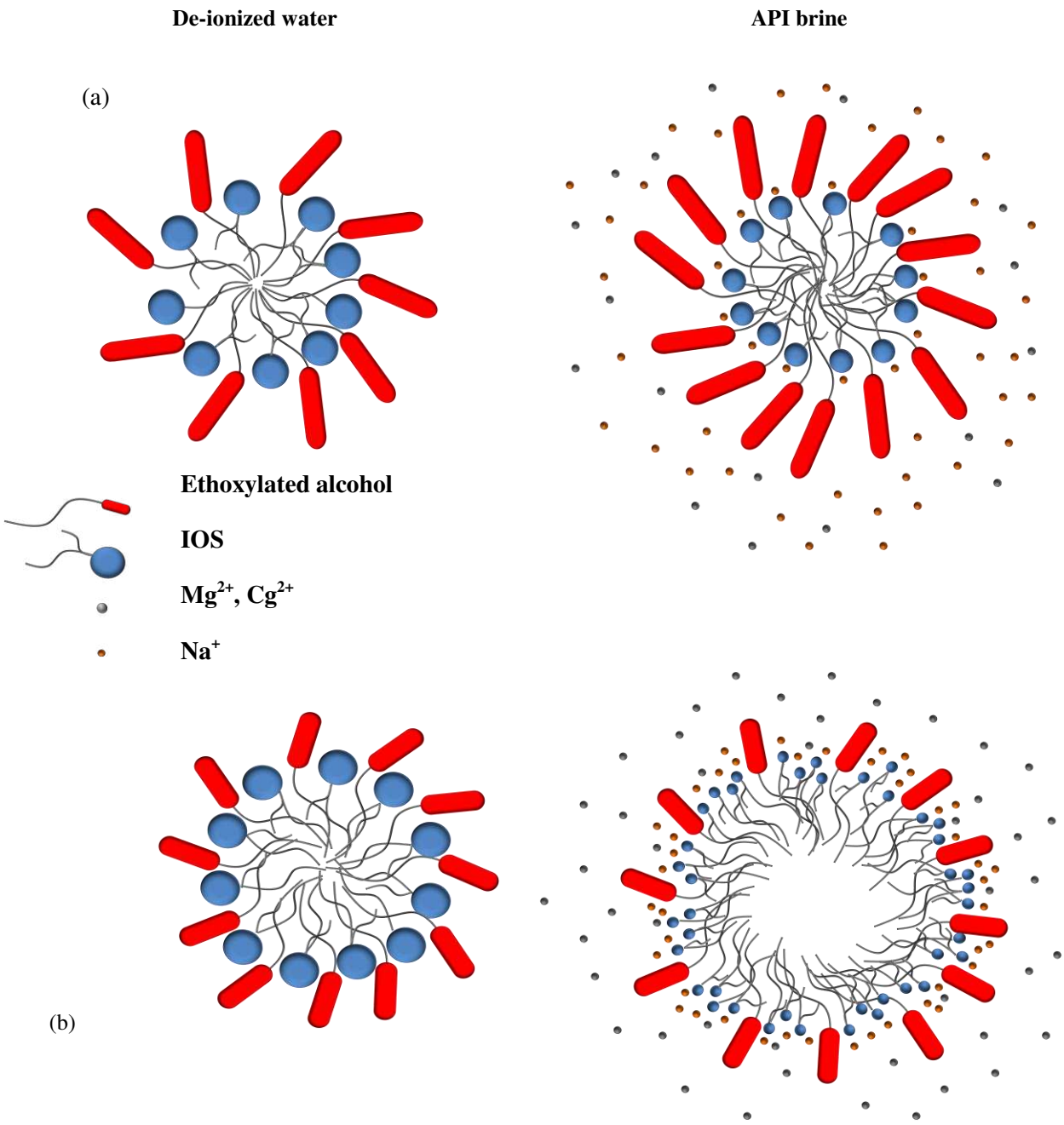

Figure 3. Schematic of mixed micelles of (a) O332-N25-12 and (b) IOS-N23-7 (pictorial representation not to the scale).

3.3. PHASE BEHAVIOR OF NANOPARTICLES DISPERSION

Figure 4 shows the phase behavior of IO NPs in API brine using and n-Octane as the oil phase at 70 ºC after a month. Two main points can be detected by attention to Figure 4: i) the volume of Winsor type III (bicontinuous oil/water phase) for O342-N23-7 is higher than other blends and ii) distribution of IO NPs between oil and API brine phase is different for surfactant blends.

Most of IO NPs were transferred to the oil phase for IOS-N23-7 blend however the intensity of transfer is lower for IOS-N91-8 blend (Figure 4). On the other hand in IOS-N25-12 blend most NPs remain in the aqueous phase. Transfer NPs to oil phase is due to the effect of salinity on surfactants, which cover the surface of NPs. For more clarification the phase behavior test was performed for NPs synthesized from de-ionized water (Figure 5). It is clear that in similar surfactant blend, the IO NPs migrate to oil phase in samples containing salt.

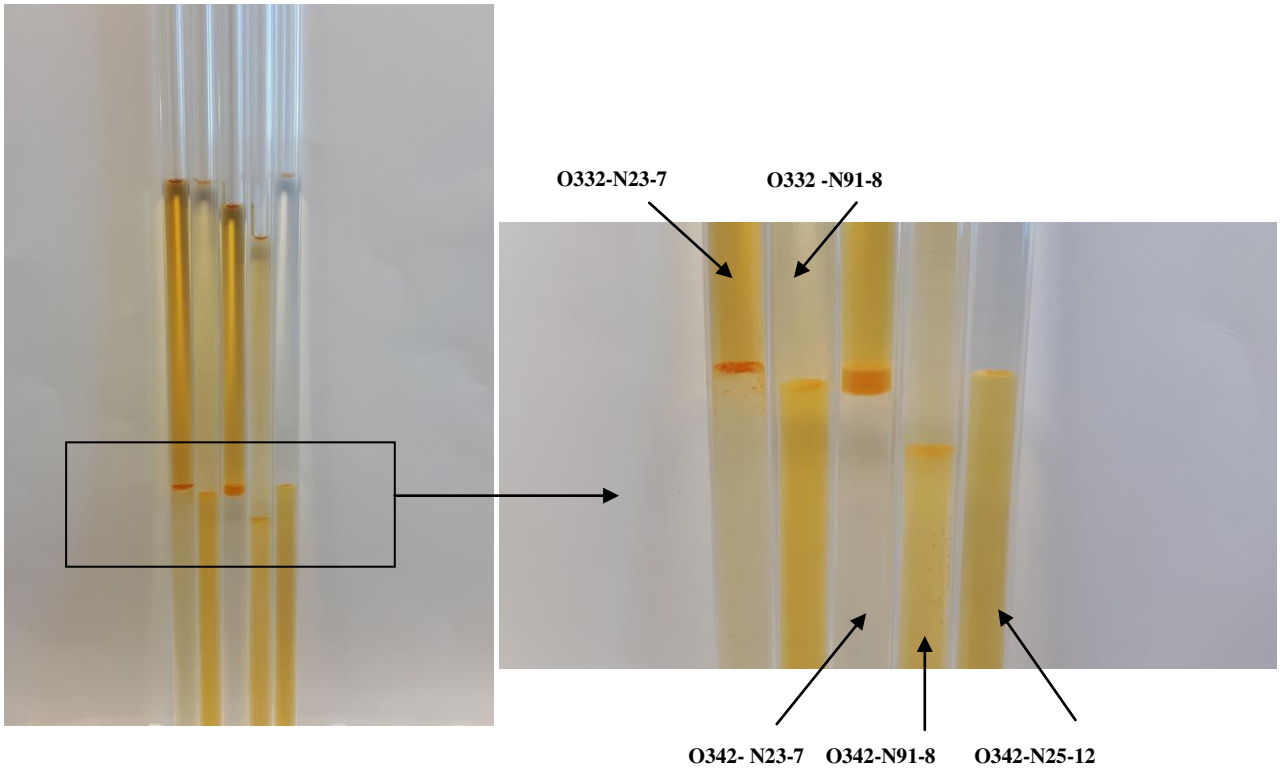

Figure 4. Phase behavior results OF nanoparticles dispersion (IO NPs in API brine) with n-Octane at 70 ºC.

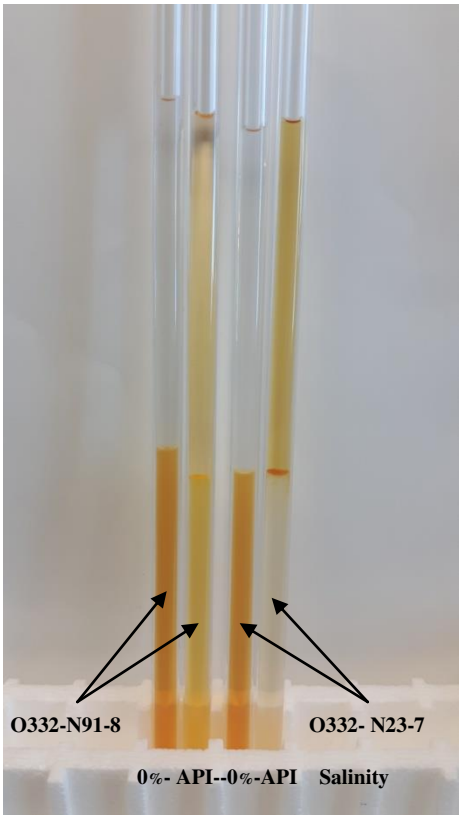

Figure 5. Effect of salinity on distribution of IO NPs in aqueous/oil phases.

The difference between IO NPs distribution intensity is related to the surface functionalizing of NPs with anionic and nonionic surfactants. Surfactants with ionic head group such as IOS are more affected in the presence of salinity compared to nonionic EA. The higher transfer of NPs to oil phase shows higher amount of IOS molecules on the surface of IO NPs. To prove this, the organic elemental analysis especially for sulfur amount in NPs was performed by the flash combustion method and EDX analysis.

Samples for elemental analysis were prepared by sedimentation of IO NPs using centrifuging of 50 mL IO NPs dispersions (500 ppm) for 1 hr at 10,000 rpm in an ultracentrifuge (Thermo Scientific megafuge 16R). The sedimented particles washed with 5 ml de-ionized water and dried in an oven for 48 hours at 80 ºC to evaporate water. Table 2 represents the results of elemental analysis of samples.

Table 2. Elemental analysis of IO NPs containing different surfactant blends.

Element	O332-N2-37	O332-N91-8	O342-N2-37	O342-N91-8	O342-N25-12
Carbon (wt. %)-Flash	3.64	3.25	3.70	3.28	3.48
Sulfur (wt. %)-Flash	1.08	0.31	1.28	0.46	0.12
Sulfur (wt. %)-EDX	1.9	1.2	2.2	1.6	1

Higher sulfur element in samples containing O342-N2-37 blends shows the higher amount of IOS molecules on the surface of IO NPs. EDX analyses were carried out from the surface of sedimented particles after coating with carbon using a pumped sputter coater (Q150T Turbo, Quorum Technologies Ltd, UK). The average value of sulfur percent for 5 different EDX areas (50×50 micron) was reported in Table 2 and an image of each sample's map was illustrated Figure S3.

3.3. PROPOSED MECHANISMS FOR STABILITY OF IO NP

The schematic proposed formation mechanism of IO NPs near mixed micelles is illustrated in Figure 6. Shorter EO group and smaller sulfonic head in IOS-N23-7 micelles provide enough space for the attachment of sulfonic group to the surface of IO NP. The appropriate ratio of anionic/nonionic surfactants at the surface of NP makes them stable on high salinity-high temperature conditions. At high salinities, EO groups at surface of NP reduce the density of divalent ions around the sulfonic group which cause the degradation of IOS molecules. On the other hand at high temperature, the sulfonic group at the surface of NP keeps the water molecules near the EO groups and prevents the dehydration of EA molecules. The IOS-EA supplements each other to produce a synergistic effect that stabilizes NP. Such synergism effect is more powerful for IOS-N23-7 blend than to the IOS-N25-12 blend, as shown in Figure 6.

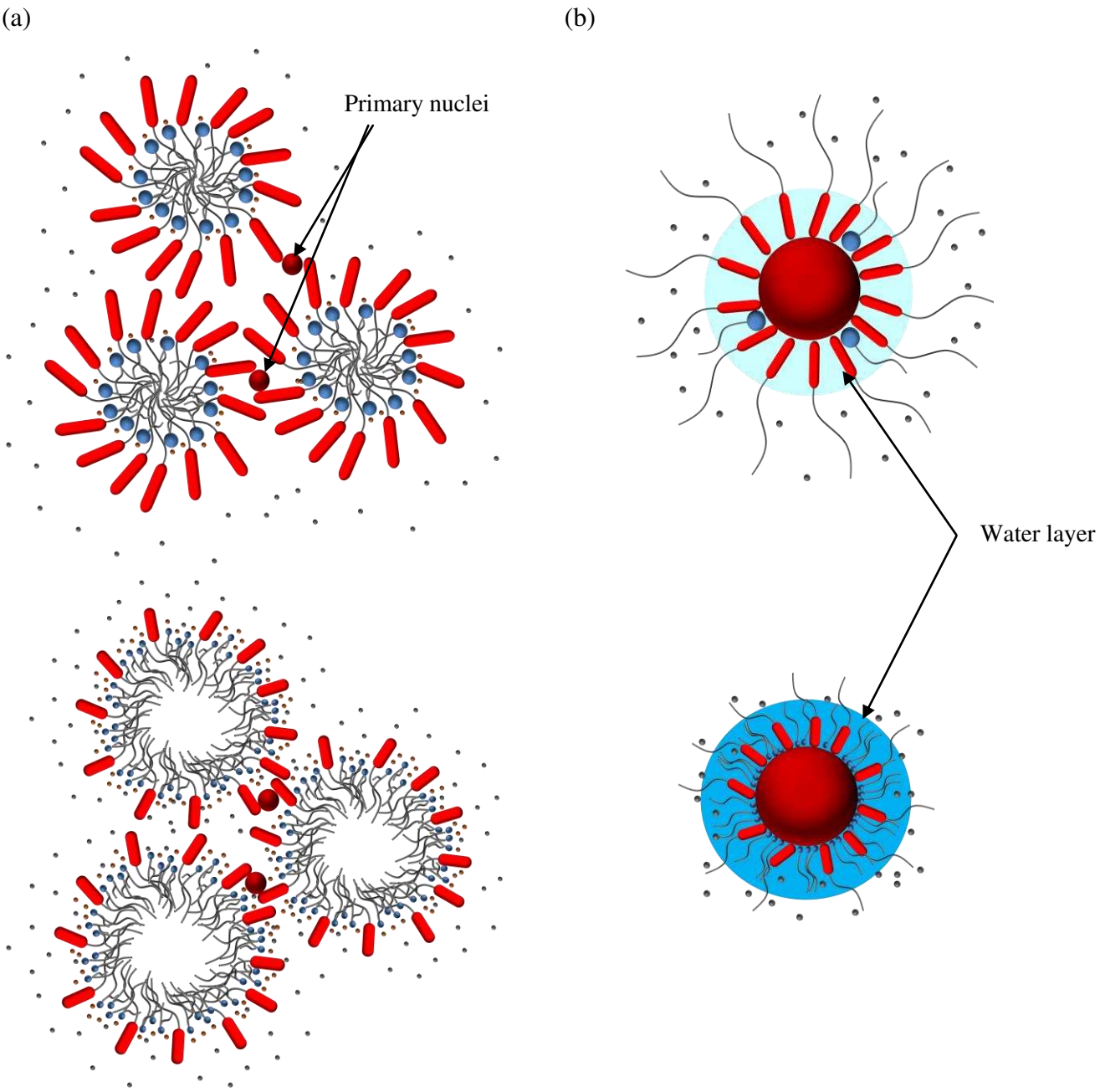

Figure 6. Schematic of IO NPs formation in micellar solution of (a) IOS-N23-7 and (b) IOS-N25-12 (pictorial representation not to the scale).

3.4.TEM ANALYSIS

The morphology and size distribution of the synthesized IO NPs in API brine containing O342-N23-7 and O342-N25-12 surfactant blends were examined by TEM (Figure 7). IO NPs

consisted mainly of globular morphologies without any agglomeration. EDX analysis of IO NPs showed a strong peak in graph at 6.2 keV (Figure 7c) corresponding to the iron element. An extra peak of carbon and cupper were observed on EDX graph, which was due to the carbon coated copper TEM grids used.

(a)

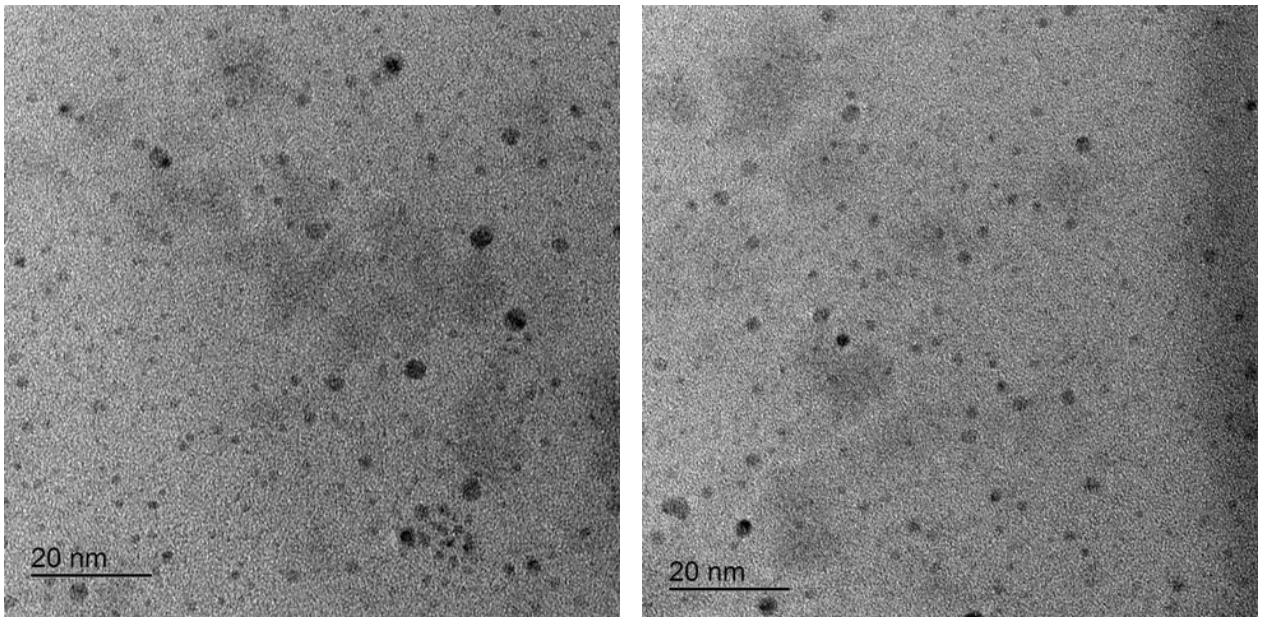

(b)

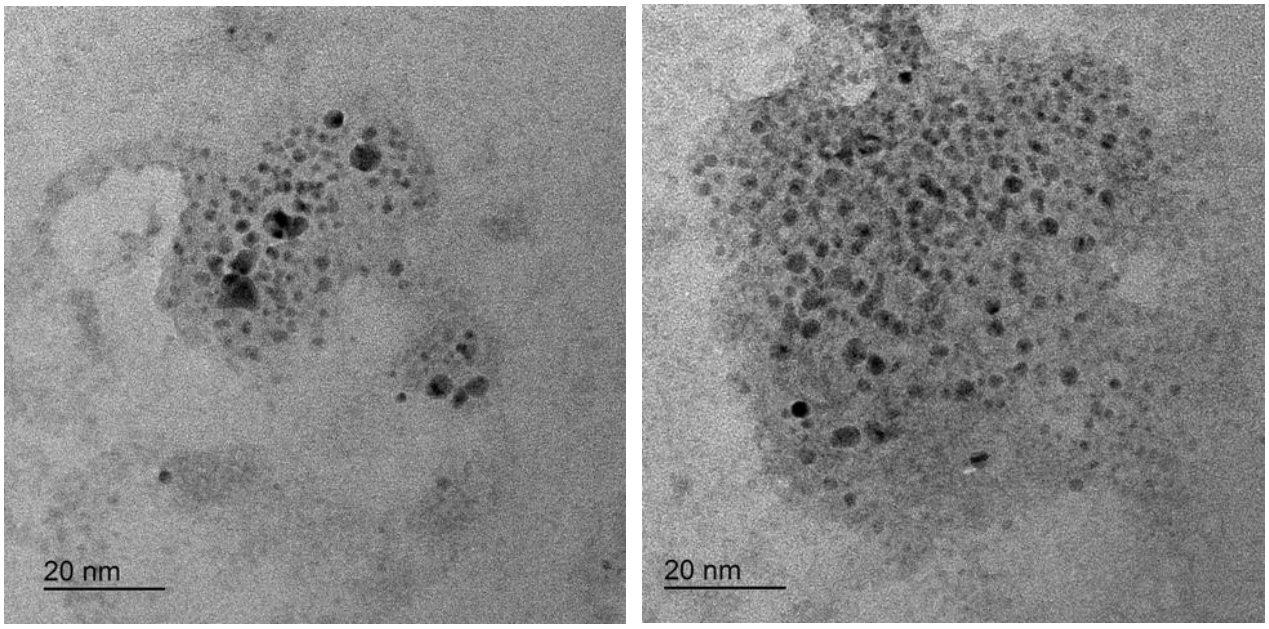

(c)

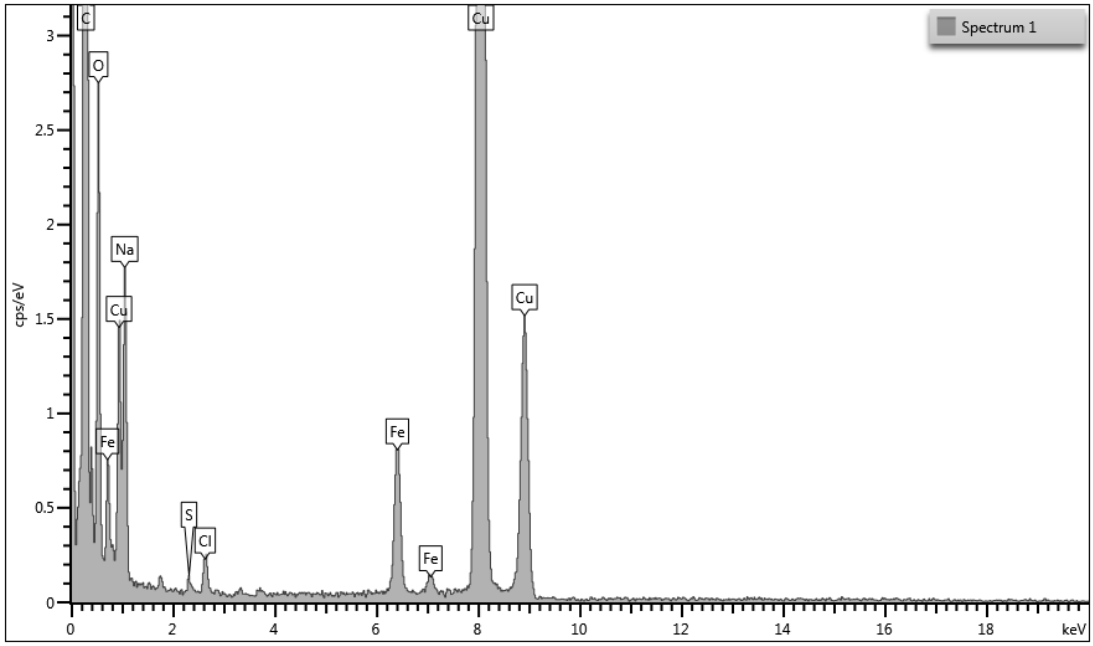

Figure 7. TEM photo of synthesized IO NPs in API brine containing (a) O342-N23-7, (b) O342-N25-12 surfactant blends and (c) EDX analysis of IO NPs in API brine containing O342-N25-12 surfactant blends.

3.5.OTHER CHARACTERIZATION ANALYSIS OF IO NP DISPERSIONS

Table 3 and 4 show the IFT of mineral oil in the presence of surfactant solutions (API brine containing 0.001 g/ml surfactant blend) and IO NPs dispersions (API brine containing 0.001 g/ml surfactant blend and 500 ppm IO NPs), respectively. It shows that IO NPs leads decreasing the IFT. Moreover IO NPs containing O342-N23-7 has the minimum IFT, which is in agreement with phase behavior results in Figure 4.

Table 3. IFT of surfactant solution containing different surfactant blends.

Surfactant mixture	O332-N23-7	O332-N91-8	O342-N25-12	O342-N23-7	O342-N91-8	O342-N25-12
IFT	4.37±0.21	2.61±0.17	2.69±0.27	4.56±0.37	3.67±0.11	4.62±0.17
Surfactant mixture	O332	O342	N23-7	N91-8	N25-12	
IFT	6.31±0.40	5.52±0.38	2.98±0.41	2.53±0.14	3.75±0.19	

Table 4. Characterization of IO NPs dispersion containing 500 ppm IO NPs.

Surfactant mixture	O332-N23-7	O332-N91-8	O342-N23-7	O342-N91-8	O342-N25-12
IFT	3.81±0.34	2.04±0.23	1.9±0.10	3.35±0.19	4.44±0.41
Average hydrodynamic size (nm)	38	95	34	49	199
Zeta	-2.21	-2.11	-3.45	-2.73	3.94
$\frac{\mu_{\exp}}{\mu_{water}}$	1.21	1.64	1.27	1.54	1.29

The hydrodynamic particle size distributions and average hydrodynamic sizes and zeta potential of IO NPs were shown in Figure 8 and Table 4 respectively. The average hydrodynamic diameter of IO NPs dispersion containing IOS-N23-7 are 34 and 38 nm respectively, which less than majority of pore throats of reservoir rocks[38]. The zeta potential value of IO NPs is a measure of electrical double layer repulsion force between NPs. According to Table 4, the zeta potential of IO NPs is between -4 and 4 mV, which suggest the presence of thin and compressed double layers around NPs. If based on pure electrostatic stabilization, nanofluid with zeta potential between 40-60 mV is typically required have an acceptable stability by electrostatic repulsion[39]. Consequently, it can be concluded that the stable functionalizing around IO NPs at high salinity-high temperature conditions is due mainly to the strong steric repulsion between particles.

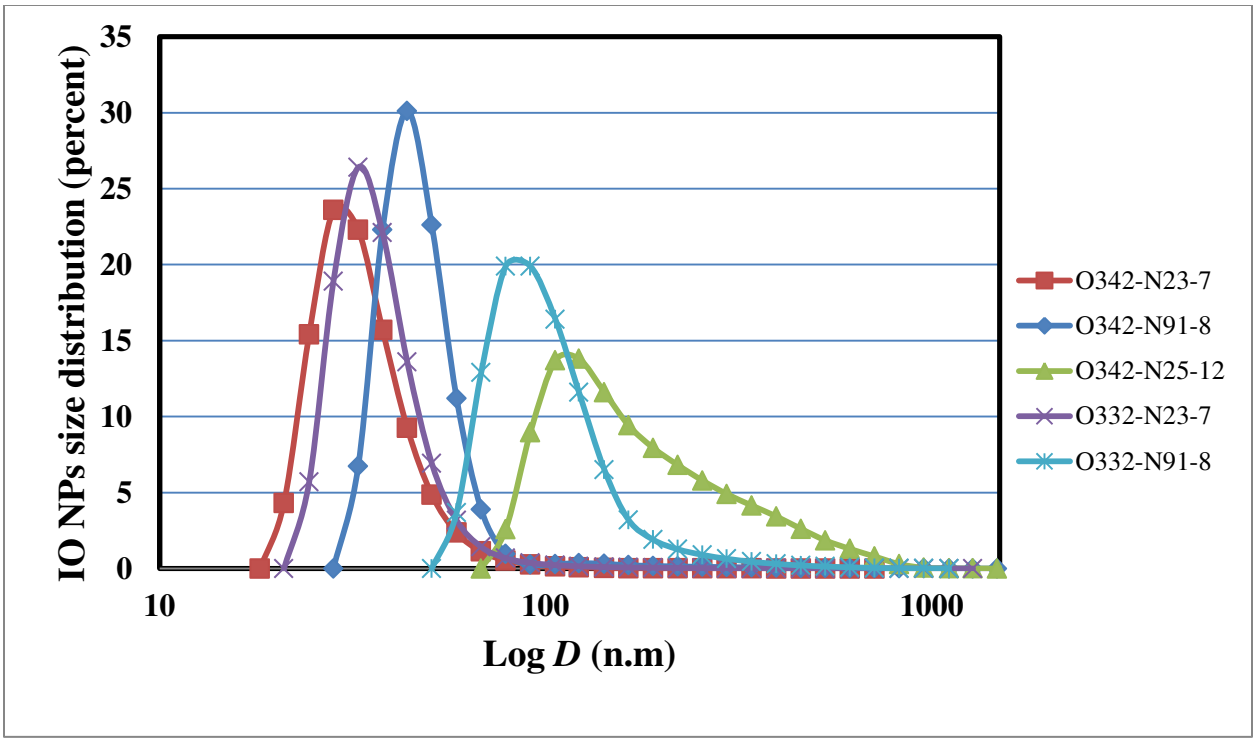

Figure 8. hydrodynamic particle size distributions of IO NPs dispersions containing different surfactant blends.

The dependence of shear stress on shear rate for different IO NPs dispersions and pure water at 22 ℃ is shown on **Error! Reference source not found.**. Despite a small intercept on the shear stress axis due to the measurement uncertainty, IO NPs dispersions clearly show a Newtonian behavior, similar to other observations[40-42]. Clearly the introduction of NPs increases the viscosity, as shown in Table 4, which shows the ratios of IO NPs dispersion viscosity (at constant shear rate of 200 s^{-1}) on pure water's viscosity (85×10^{-4} Pa.s) were presented. The higher viscosity of IO NPs dispersion compare to water is an advantage for oil recovery process by improving the mobility ratio.

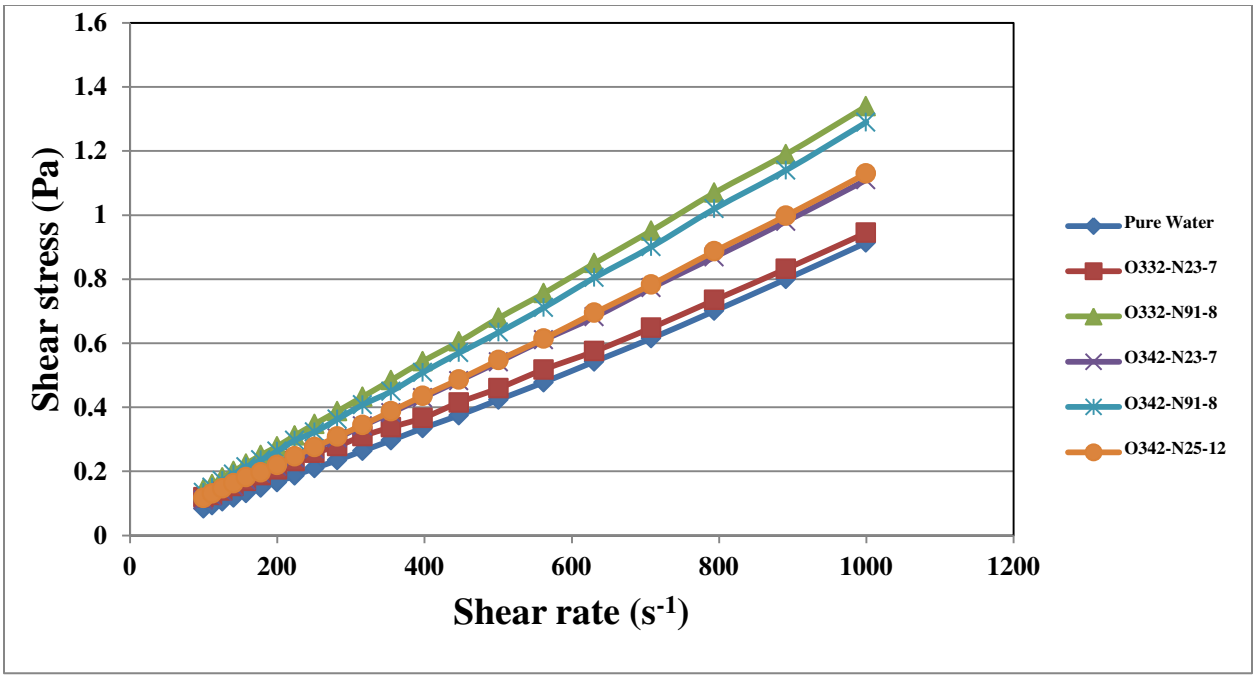

Figure 9. Rheological curve of IO NPs dispersion.

Conclusion

This work confirms the novel strategy to synthesize stable nanoparticles under harsh conditions by using the synergistic effect of a surfactant mixture. Long-term stable IONPs were produced in API brine containing 2 wt% of $MgCl_2$ at 70 ºC. Mixed micelles of internal olefin sulfonate (IOS) and ethoxylated alcohol (EA) produced a synergistic effect for the stabilization of NPs at high salinity-high temperature conditions. IOS have chemical stability at higher temperatures (up to 150°C) because of sulfonate hydrophilic head group, which keep holding water molecules at high temperature. On the other hand EA has not been influenced at high salinity and keep away counterions form hydrophilic head of IOS. The phase behavior experiments showed that IONPs were transferred to the oil phase because of the effect of salinity on surfactants, which covers the surface of NPs. Surfactants with ionic head group such as IOS are more affected in the presence of salinity compared to nonionic EA. Distribution of IONPs in oil phase is dependent on the ratio of anionic/nonionic surfactants on the surface of functionalized NPs. The results show that IONPs, which has been synthesized in the O334-N23-7 blend have higher stability because of the optimized synergistic effect. Moreover, the

combined stability and desirable interfacial and rheology properties show the promise for EOR applications.

Corresponding Author

*E-mail: d.wen@leeds.ac.uk

ACKNOWLEDGEMENT

The authors thank Mr. Paul Kunkeler (Shell Chemicals Europe) for generously providing us their commercial surfactant EOR products. This work was supported by European Research Council Consolidator Grant (Grant number: 648375).

REFERENCES

(1) Cheraghian, g.; L. Hendraningrat, L. A review on applications of nanotechnology in the enhanced oil recovery part A: effects of nanoparticles on interfacial tension. *Int. Nano. Lett.* **2016** 6 (2), 129-138.

(2) Wei, B.; Li, Q.; Jin, F.; Li, H.; Wang, C. The Potential of a Novel Nanofluid in Enhancing Oil Recovery. *Energy Fuels*. **2016**, 30 (4), 2882–2891

(3) Hendraningrat, L.; Li, S.; Torsaeter, O. A coreflood investigation of nanofluid enhanced oil recovery. *J. Pet. Sci. Eng*. **2013**, 111, 128-138.

(4) Esfandyari Bayat, A.; Junin, R.; Samsuri, A.; Piroozian, A.; Hokmabadi, M. Impact of Metal Oxide Nanoparticles on Enhanced Oil Recovery from Limestone Media at Several Temperatures. *Energy Fuels*. **2014,** 28 (10) 6255-6266.

(5) Yoon, K. Y. *The Design and Control of Stability and Magnetic Properties of Imaging Nanoparticles*; Doctor of Philosophy dissertation, University of Texas at Austin, 2012.

(6) Kini, G. C.; Yu, J.; Wang, L.; Kan, A. T.; Biswal, S. L.; Tour, J. M.; Tomson, M. B.; Wong, M. S. Salt and Temperature Stable Quantum Dot Nanoparticles for Porous Media Flow. *Colloids. Surf. A.* **2014**, 443, 492-500.

(7) Rahmani, A. R.; Bryant, S. L.; Huh, C.; Ahmadian, M.; Zhang, W.; Liu Q. H. *Characterizing Reservoir Heterogeneities Using Magnetic Nanoparticles*; SPE Reservoir Simulation Symposium, Texas, USA, 2015.

(8) Lim, J. K.; Majetich, S. A.; Tilton, R. D. Stabilization of Superparamagnetic Iron Oxide Core-Gold Shell Nanoparticles in High Ionic Strength Media. *Langmuir*. **2009**, 25 (23), 13384-13393.

(9) Bagaria, H. G.; Yoon, K. Y.; Neilson, B. M.; Cheng, V.; Lee, J. H.; Worthen, A. J.; Xue, Z.; Huh, C.; Bryant, S. L.; Bielawski, C. W.; Johnston, K. P. Stabilization of Iron Oxide Nanoparticles in High Sodium and Calcium Brine at High Temperatures with Adsorbed Sulfonated Copolymers. *Langmuir*, **2013**, 29 (10), 3195-3206.

(10) Bagaria, H. G.; Xue, Z.; Neilson, B. M.; Worthen, A. J.; Yoon, K. Y.; Nayak, S.; Cheng, V.; Lee, J. H.; Bielawski, C. W.; Johnston, K. P. Iron Oxide Nanoparticles Grafted with Sulfonated Copolymers are Stable in Concentrated Brine at Elevated Temperatures and Weakly Adsorb on Silica. *ACS Appl. Mater. Interfaces*. **2013**, 5 (8), 3329-3339.

(11) Ranka, M.; Brown, P.; Hatton, T. A. Responsive Stabilization of Nanoparticles for Extreme Salinity and High-Temperature Reservoir Applications. *ACS Appl. Mater. Interfaces.* **2015**, 7 (35), 19651-19658.

(12) Barnes, J. R.; Groen, K.; On, A.; Dubey, S. T.; Reznik, C.; Buijse, M. A.; Rijswijk, B. V.; Shepherd, A. G. *Controlled Hydrophobe Branching to Match Surfactant to Crude Oil Composition for Chemical EOR*; 18th SPE Improved Oil Recovery Symposium, Oklahoma, USA, 2012.

(13) Wu, Y.; Shuler, P.; Blanco, M.; Tang, Y.; Goddard, W. A. *A Study of Branched Alcohol Propoxylate Sulfate Surfactants for Improved Oil Recovery*. SPE Annual Technical Conference and Exhibition, Dallas, Texas, 2005.

(14) Jang, S. H.; Liyanage, P. J.; Lu, J.; Kim, D. H.; Pinnawala Arachchilage, G. W. P.; Britton, C; Weerasooriya, U; Pope, G. A. *Microemulsion Phase Behavior Measurements Using Live Oils at High Temperature and Pressure*. SPE Improved Oil Recovery Symposium, Oklahoma, USA, 2014.

(15) Puerto, M. C.; Hirasaki, G. J.; Miller, C. A.; Reznik, C.; Dubey, S.; Barnes, J. R.; Van Kuijk, S. *Effects of Hardness and Cosurfactant on Phase Behavior of Alcohol-Free Alkyl Propoxylated Sulfate Systems*. SPE 169096-MS, SPE Improved Oil Recovery Symposium, Oklahoma, USA, 2014.

(16) Barnes, J. R.; Smit, J. P.; Shpakoff, P. G.; Raney, K. H.; Puerto, M. C. *Phase Behaviour Methods for the Evaluation of Surfactants for Chemical Flooding at Higher Temperature Reservoir Conditions*. SPE Improved Oil Recovery Symposium, Oklahoma, USA., 2008.

(17) Fujimoto, T. *New Introducing to Surface Active Agents*. Kyoto, Japan: Sanyo Chemical Industries Ltd., 1985.

(18) Muherei, M. A.; Junin, R. Mixing Effect of Anionic and Nonionic Surfactants on Micellization. *Mod. Appl. Sci.* **2008**, 2, 3-12.

(19) Salanger, J. L. *Surfactants-Types and Uses*. Laboratorio FIRP, Merida, Venezuela, 1999.

(20) Zarate Munoz, S.; Troncoso, A. B.; Acosta, E.; The Cloud Point of Alkyl Ethoxylates and Its Prediction with the Hydrophilic-Lipophilic Difference (HLD) Framework. *Langmuir.* **2015**, 31 (44), 12000-12008.

(21) Puerto, M.; Hirasaki, G. J.; Miller, C. A.; Barnes, J. R. *Surfactant Systems for EOR in High-Temperature, High-Salinity Environments*. SPE Symposium on Improved Oil Recovery, Tulsa, 2010.

(22) Abe, M.; Schechter, D.; Schechter, R. S.; Wade, W. H.; Weerasooriya, U.; Yiv, S. Microemulsion formation with branched tail polyoxyethylene sulfonate surfactants. *J. Colloid Interface Sci.* **1986** ,114 (2), 342-356.

(23) Bansal V. K.; Shah, D. O. The Effect of Ethoxylated Sulfonates on Salt Tolerance and Optimal Salinity of Surfactant Formulations for Tertiary Oil Recovery. *SPE J.* **1978**, 18 (3), 167-172.

(24) Bansal V. K.; Shah, D. O. The effect of addition of ethoxylated sulfonate on salt tolerance, optimal salinity, and impedence characteristics of petroleum sulfonate solutions. *J. Colloid and Interface Sci.* **1978**, 65 (3), 451-459.

(25) Bera, A.; Mandal, A.; Guha, B. B. Synergistic Effect of Surfactant and Salt Mixture on Interfacial Tension Reduction between Crude Oil and Water in Enhanced Oil Recovery. *J. Chem. Eng. Data*. **2014,** 59 (1), 89-96.

(26) Li, Y.; Zhang, W.; Kong, B.; Puerto, M.; Bao, X.; Sha, O.; Shen, Z; Yang, Y.; Liu, Y.; Gu, S.; Miller, C.; Hirasaki, G. J. *Mixtures of Anionic-Cationic Surfactants: A New Approach for Enhanced Oil Recovery in Low-Salinity, High-Temperature Sandstone Reservoir*. SPE Improved Oil Recovery Symposium, Oklahoma, USA, 2014.

(27) Massart, R. Preparation of aqueous magnetic liquids in alkaline and acidic media. *IEEE Trans. Magn.* **1981**, 17 (2), 1247-1248.

(28) You, Y.; Wu, X.; Zhao, J.; Ye, Y.; Zou, W. Effect of alkyl tail length of quaternary ammonium gemini surfactants on foaming properties. *Colloids and Surfaces A: Physicochem. Eng. Aspects.* **2011**, 384 (1-3), 164-171.

(29) Salaniwal, S.; Kumar, S. K.; Panagiotopoulos, A. Z. Competing Ranges of Attractive and Repulsive Interactions in the Micellization of Model Surfactants. *Langmuir.* **2003,** 19 (12), 5164-5168.

(30) Shell Company. http://www.shell.com/business-customers/chemicals/our-products/higher-olefins-and derivatives/enordet-surfactants.html.

(31) Schluter, B.; Mulhaupt, R.; Kailer, A. Synthesis and Tribological Characterization of Stable Dispersions of Thermally Reduced Graphite Oxide. *Tribol. Lett.* **2014**, 53 (2014), 353-363.

(32) Zhang, H.; Li, Y.; Dubin, P.; Kato, T. Effect of EO Chain Length of Dodecanol Ethoxylates ($C_{12}E_n$) on the Complexation of $C_{12}E_n$/SDS Mixed Micelles with an Oppositely Charged Polyelectrolyte. *J. Colloid Interface Sci.* **1996**, 183 (2), 546-551.

(33) Aswal, V. K.; Goyal, P. S. Dependence of the size of micelles on the salt effect in ionic micellar solutions. *Chem. Phys. Lett.* **2002**, 364 (1-2), 44-50.

(34) Horiuchi , S.; Winter, G. CMC determination of nonionic surfactants in protein formulations using ultrasonic resonance technology. *Eur. J. Pharm. Biopharm*. **2015**, 92, 8-14.

(35) Manzo, G.; Carboni, M.; Rinaldi, A. C.; Casu, M.; Scorciapino, M. A. Characterization of sodium dodecylsulphate and dodecylphosphocholine mixed micelles through NMR and dynamic light scattering. *Magn. Reson. Chem*. **2013**, 51 (3), 176-183.

(36) Malvern Instruments Ltd. *Surfactant Micelle Characterization using Dynamic Light Scattering*, Zetasizer Nano Application Note, MRK809-01, 2006.

(37) Klose, G.; Eisenblaetter, S.; Galle, J.; Islamov, A.; Dietrich, U. Hydration and Structural Properties of a Homologous Series of Nonionic Alkyl Oligo (ethylene oxide) Surfactants. *Langmuir*. **1995**, 11 (8), 2889-2892.

(38) Nelson, P. H. Pore-throat sizes in sandstones, tight sandstones, and shales. AAPG *Bulletin*. **2009**, 93 (3), 329-340.

(39) Mukherjee, S.; Paria, S. Preparation and Stability of Nanofluids-A Review. *IOSR-JMCE*. **2013**, 9 (2), 63-69.

(40) Tang, C. C.; Tiwari, S.; Cox, M. W. Viscosity and Friction Factor of Aluminum Oxide–Water Nanofluid Flow in Circular Tubes. *J. Nanotechnol. Eng. Med*. **2013**, 4 (2), 1-6.

(41) Fedele, L.; Colla, L.; Bobbo, S. Viscosity and thermal conductivity measurements of water-based nanofluids containing titanium oxide nanoparticles. *Int. J. Refrig.* **2012**, 35 (5), 1359-1366.

(42) Tadjarodi, A.; Zabihi, F. Thermal conductivity studies of novel nanofluids based on metallic silver decorated mesoporous silica nanoparticles. *Mater. Res. Bull.* **2013**, 48 (10), 4150 – 4156.